Structure and Infrastructure Engineering, Vol. 3, No. 2, June 2007, 103 – 120

Taylor & Francis
Taylor & Francis Group

A wireless structural health monitoring system with multithreaded sensing devices: design and validation

YANG WANG†, JEROME P. LYNCH‡ and KINCHO H. LAW*†

†Department of Civil and Environmental Engineering, Stanford University, Stanford, CA 94305-4020, US
‡Department of Civil and Environmental Engineering, University of Michigan, Ann Arbor, MI 48109, US

(*Received 16 April 2005; accepted in revised form 8 September 2005*)

Structural health monitoring (SHM) has become an important research problem which has the potential to monitor and ensure the performance and safety of civil structures. Traditional wire-based SHM systems require significant time and cost for cable installation. With the recent advances in wireless communication technology, wireless SHM systems have emerged as a promising alternative solution for rapid, accurate and low-cost structural monitoring. This paper presents a newly designed integrated wireless monitoring system that supports real-time data acquisition from multiple wireless sensing units. The selected wireless transceiver consumes relatively low power and supports long-distance peer-to-peer communication. In addition to hardware, embedded multithreaded software is also designed as an integral component of the proposed wireless monitoring system. A direct result of the multithreaded software paradigm is a wireless sensing unit capable of simultaneous data collection, data interrogation and wireless transmission. A reliable data communication protocol is designed and implemented, enabling robust real-time and near-synchronized data acquisition from multiple wireless sensing units. An integrated prototype system has been fabricated, assembled, and validated in both laboratory tests and in a large-scale field test conducted upon the Geumdang Bridge in Icheon, South Korea.

Keywords: Structural monitoring; Wireless sensing; Sensor networks; Data acquisition; On-board data processing; Vibration tests

1. Introduction

The safety and reliability of civil infrastructure systems are essential for supporting the economic vitality of our society. As civil structures are continuously subjected to loads and other environmental effects, the structural condition of many civil infrastructures in the US is deteriorating. For example, more than half of the bridges in the US were built before the 1940s, and nearly 42% of them were reported to be structurally deficient and below established safety standards (Stallings *et al*. 2000). To protect the public from unsafe bridge structures, current US federal requirements necessitate local transportation authorities to visually inspect the entire inventory of well over 580,000 highway bridges biannually (Chase 2001). An inherent drawback of visual inspections is that they only consider damage that is visible on the surface of the structure; damage located below the surface often remains elusive to the inspectors. Furthermore, bridge inspections can be highly subjective. For example, a recent study by the US Federal Highway Administration (FHWA) quantified the reliability of visual inspections with wide variability discovered in the condition ratings assigned by trained inspectors to a bridge intentionally damaged as part of the study (Moore *et al*. 2001). With visual inspections both costly and labor intensive, low cost sensing systems that can quantitatively assess the integrity and remaining life of a structure are needed (Liu *et al*. 2003).

*Corresponding author. Email: law@stanford.edu

Structure and Infrastructure Engineering
ISSN 1573-2479 print/ISSN 1744-8980 online © 2007 Taylor & Francis
http://www.tandf.co.uk/journals
DOI: 10.1080/15732470600590820

As a complimentary approach and promising alternative to visual structural inspections, structural health monitoring (SHM) systems have been proposed to predict, identify, and locate the onset of structural damage (Sohn *et al*. 2001, Chang *et al*. 2003, Elgamal *et al*. 2003). SHM systems employ smart sensor technologies to assist in identifying subtle structural abnormalities based on measured structural response parameters (Farrar *et al*. 2003, Spencer *et al*. 2004). Various types of structural sensors, including accelerometers, displacement transducers, strain gages, and thermometers, can be deployed to provide valuable real-time information about the behavior of a structure or environmental conditions. A necessary element of a SHM system is the data acquisition (DAQ) system used to collect sensor measurements and to store the data in a centralized location. Current commercial DAQ systems designed for permanent installation or for short-term vibration tests employ cables to directly transmit sensor data to the central data repository. By running cables between sensors and the data server, traditional DAQ systems suffer from high installation costs in terms of both time and money. Installing extensive lengths of cables can consume over 75% of the total SHM system installation time (Straser and Kiremidjian 1998). In the US, the cost of installing a typical structural monitoring system in buildings can exceed a few thousand dollars per sensing channel (Celebi 2002).

Recent developments in the fields of microelectromechanical systems (MEMS) and wireless communications have introduced new opportunities to reduce the installation costs of structural monitoring systems (Min *et al*. 2001, Warneke *et al*. 2002, Lynch *et al*. 2004b). MEMS technology has led to the development of sensors that are low cost, low power, compact, and easy to install; while wireless technology allows for transmitting sensor measurements without the need for cables. The use of wireless communications as a means for eradicating cables within a structural monitoring system was illustrated by Straser and Kiremidjian (1998). Their work demonstrated both the feasibility and the cost-effectiveness of wireless SHM systems. With respect to the architectural design of wireless SHM systems, Kottapalli *et al*. (2003) proposed a two-tiered wireless sensor network topology that especially addressed the power consumption, data rate, and communication range limitations of current wireless monitoring systems. Lynch *et al*. (2004a) explored further the concept of embedding damage identification algorithms directly into wireless sensing units, harnessing the computational resources of these devices to execute data interrogation algorithms. The embedment of engineering algorithms within the wireless sensing units serves as a means of reducing power-consuming wireless communications, and thereby largely improves the scalability of the system. Many other research efforts in developing wireless sensing platforms for structural health monitoring have been reported (Hill 2003, Kling 2003, Arms *et al*. 2004, Callaway 2004, Culler *et al*. 2004, Glaser 2004, Mastroleon *et al*. 2004, Ou *et al*. 2004, Shinozuka *et al*. 2004, Spencer *et al*. 2004).

Compared to traditional wire-based systems, wireless structural monitoring systems have a unique set of technical challenges (Wang *et al*. 2005b). First, wireless sensing units will most likely employ batteries that have a limited supply of energy for the near future. Batteries are probable in the short-term because current power harvesting techniques cannot yet provide a reliable, convenient, and low-cost solution for powering typical wireless structural sensors (Churchill *et al*. 2003, Roundy 2003, Sodano *et al*. 2004). In terms of power consumption, wireless transceivers often consume the greatest amount of energy than any of the other components in the wireless sensor design (Lynch *et al*. 2004a). Local data processing targeted to balance data transmission and energy consumption is desirable. Secondly, the transmission of data in a wireless network is inherently less reliable than in cable-based networks; reliability decreases as the communication range becomes further. Thirdly, the limited amount of wireless bandwidth usually impedes high-speed real-time data collection from multiple sensors. Fourthly, time delays encountered during data transmission between different wireless sensing units due to sensor blockage or clock imprecision needs to be thoroughly considered (Lei *et al*. 2003).

The wireless structural monitoring system proposed in this paper attempts to address some of the technical challenges described above. The design of this new system was especially oriented for large-scale and low-power wireless SHM applications in civil structures (Wang *et al*. 2005a). Some of the main features of this new wireless SHM system are: (1) low power consumption while achieving long communication ranges with robust communication protocols for reliable data acquisition, (2) accurate synchronized wireless data collection from multiple analog sensors at a reasonable sampling rate suitable for civil structural applications, (3) high-precision analog-to-digital conversion, (4) considerable local data processing capability at the wireless sensing units to reduce energy consumption and to enhance system scalability, and (5) accommodation of peer-to-peer communication among wireless sensing units for collaborative decentralized data analysis. An integrated wireless SHM system has been developed, fabricated and assembled. Furthermore, the SHM system has undergone laboratory and large-scale field tests to validate the system performance within the complex environment posed by civil structures. The field tests were conducted at Geumdang Bridge in Icheon, South Korea by simultaneously employing 14 wireless sensing units on the bridge for continuous real-time data acquisition using a single data server (Lynch *et al*. 2005).

This paper presents in detail the hardware organization of this new wireless SHM system. Major circuit components of the wireless sensing units are introduced, with key hardware performance features of the system summarized. Various aspects of the system software design are also described. A state machine design concept is employed in developing a robust communication protocol for the wireless SHM system. The software mechanism that enables near-synchronized real-time data acquisition simultaneously from multiple wireless sensing units is also described herein. Embedded computing algorithms executed by the wireless sensing unit illustrate the potential for local data processing within a wireless sensor network. Finally, the paper presents both laboratory and field tests intended to accurately assess the performance merits and weaknesses of the integrated hardware and software SHM system proposed.

2. Hardware design of a wireless sensing unit

The prototype SHM system incorporates an integrated hardware and software design to implement a simple star-topology wireless sensor network (Callaway 2004). A wireless SHM system with a star-topology includes multiple wireless sensing units assembled in a network with one central server coordinating the activities of the network. In our prototype implementation, the central server can be a laptop or desktop computer connected with a compatible wireless transceiver through a typical RS232 serial communication port. Using the wireless transceiver, the central server can communicate with the wireless sensing units that are dispersed throughout the structure. The wireless sensing units are responsible for acquiring sensor measurements, analyzing data, and transferring data to the central server for permanent storage or further data interrogation. The functional properties of the global SHM system depend on the hardware design of the individual wireless sensing units. As discussed earlier, some of the key issues considered in the hardware design of the wireless sensing units include limited power consumption, long peer-to-peer communication ranges, and local data processing capability. These issues pose the major challenges addressed in the hardware design of the novel wireless SHM system proposed in this study.

A functional diagram of the proposed wireless sensing unit is illustrated in figure 1. The design of the wireless sensing unit consists of three functional modules: the sensing interface, the computational core, and the wireless communication channel. The sensing interface converts analog sensor signals into a digital format usable by the computational core. The digitized sensor data is then transferred to the computational core through a high-speed Serial Peripheral Interface (SPI) port. Besides a low-power 8 bit Atmel ATmega128 microcontroller, external Static Random Access Memory (SRAM) is integrated with the computational core to accommodate local data storage and analysis. Through a Universal Asynchronous Receiver and Transmitter (UART) interface, the computational core communicates with the MaxStream 9XCite wireless transceiver, which provides a wireless connection between the unit and other wireless devices or between the unit and the central server. The 9XCite operates on the unlicensed 900 MHz radio frequency spectrum and can achieve communication ranges of 300 m in open space and 90 m in an indoor environment. This section describes in detail the hardware design of each functional module of the wireless sensing unit, and summarizes the corresponding performance properties of the wireless SHM system.

2.1 *Sensing interface*

Each wireless sensing unit represents an autonomous node within the wireless monitoring system, collecting and analyzing measurements from multiple sensors. In the sensing interface module of each unit, a four-channel, 16 bit and 100 kHz analog-to-digital (A/D) converter, Texas Instrument ADS8341, is employed for converting analog sensor signals into digital data that can be recognized by the microcontroller. Any analog sensor signal between 0 and 5 V can be accepted by the A/D converter, so that the

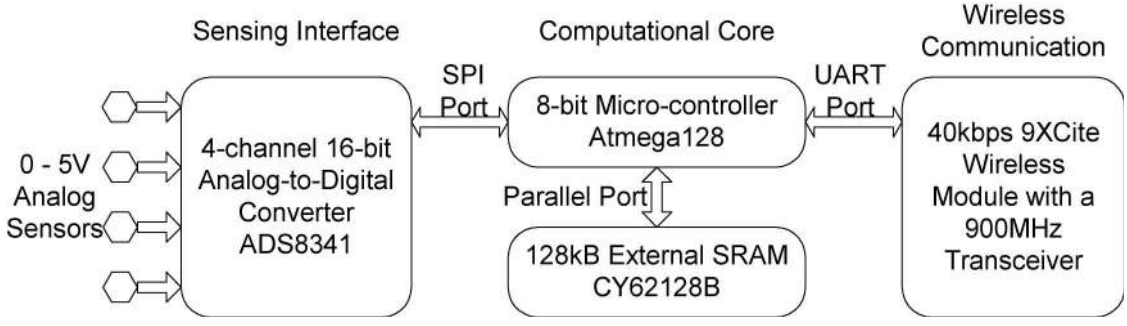

Figure 1. Functional diagram detailing the hardware design of the wireless sensing unit.

sensing unit is sufficiently generic for accommodating a heterogeneous set of analog sensors. The A/D converter can be interfaced with up to four sensors at the same time with its 16 bit resolution providing adequate accuracy for most applications in structural health monitoring. The upper limit for the sampling rate of this A/D converter is 100 kHz, which means each A/D conversion takes a very short period of time (10 μs). Therefore, each A/D conversion can be finished swiftly through the timer interrupt service of the ATmega128 microcontroller, without disrupting the UART communication between the microcontroller and the wireless transceiver. This means that it is possible for the wireless sensing unit to keep its wireless communication module functioning, even when the unit is sampling data from the sensing interface.

2.2 *Computational core*

For the computational core of the wireless sensing unit, a low-power microcontroller is employed to coordinate all of the different parts of the sensing unit hardware, and to provide the capability for local data interrogation. A low-cost 8 bit Atmel AVR microcontroller, ATmega128, is selected in this design. The ATmega128 microcontroller provides 128 kB of in-system reprogrammable flash memory, which is sufficient for storing embedded programs for many typical computational algorithms, such as fast Fourier transforms (FFT), wavelet transforms, and various other algorithms (Lynch *et al*. 2003, 2004). When the microcontroller is running at a system clock of 8 MHz, it consumes about 15 mA of current at a power supply of 5 V. The 64-pin ATmega128 provides UART/SPI communication interfaces, timer modules, interrupt modules and multiple input/output ports. Its timer and interrupt modules are used to command the A/D conversion at user-specified sampling rates. The 4 kB SRAM integrated in the microcontroller is insufficient for sensor data storage and analysis; therefore, the microcontroller is interfaced with an external 128 kB memory chip, Cypress CY62128B. Although there is a limitation of the ATmega128 microcontroller to only allow accessing 64 kB of external memory at a time, it is still possible to make full use of the 128 kB external memory by controlling a separate line that selects the lower half 64 kB or upper half 64 kB of the CY62128B chip. The external memory is sufficient for executing many sophisticated damage identification algorithms on a large quantity of sensor data.

To coordinate the behavior of the wireless sensing unit, embedded system software is written for the ATmega128 microcontroller. The embedded system software encapsulates the lower level details of the unit hardware, so that these modularized functions can be conveniently employed for upper level software development. An attractive feature of the implemented embedded software is that it can execute two tasks in parallel (multithreaded tasking). In particular, the unit is capable of collecting data from the sensing interface and simultaneously performing another operational task, such as transferring data over the wireless transceiver or executing a computational algorithm to interrogate sensor data. The multi-task execution is made possible because of the timer interrupt service provided by the ATmega128 microcontroller and the very short A/D conversion time. The interrupt function is a powerful feature that allows the software to momentarily pause an executing task (such as data processing or wireless communication) when it is the scheduled time to sample data from the sensing interface. After servicing the sensing interface, the paused task is immediately resumed.

2.3 *Wireless communication*

Robust data communication between sensors and between sensors and the data repository is important in structural health monitoring applications. For civil structures, the anticipated communication range could be upwards of several hundred meters. However, long communication ranges usually require higher power consumption on the part of the wireless transceiver. In this study, the MaxStream 9XCite wireless transceiver is selected for the wireless sensing unit because of its capability for providing relatively long range communication yet only consuming a modest amount of battery energy. This wireless transceiver offers the trade-off and balance between low power consumption and long communication distance for applications in structural health monitoring.

The key performance characteristics of the 9XCite wireless transceiver are summarized in table 1. As specified, the 90 m indoor and 300 m outdoor communication range of the 9XCite wireless transceiver is sufficient for most small and medium-sized civil structures. Meanwhile, the 9XCite transceiver consumes a current of only about 50 mA when

Table 1. Key characteristics of the MaxStream 9XCite wireless transceiver.

Specification	Transceiver parameter
Communication range	Up to 300′ (90 m) indoor, 1000′ (300 m) outdoor
Data transfer rate	38.4 kbps
Operating frequency	902 – 928 MHz
Channel mode	7 channels at Frequency Hopping Spreading Spectrum (FHSS) mode, or 25 channels at Single Frequency mode
Supply voltage	2.85 VDC to 5.50 VDC
Power consumption	55 mA transmitting, 35 mA receiving, 20 μA standby
Module size	$1.6 \times 2.825 \times 0.35''$ ($4.06 \times 7.17 \times 0.89$ cm)
Network topology	Point-to-point, point-to-multipoint

transmitting data, or a current of about 30 mA when receiving data. A much lower current is consumed when the 9XCite transceiver is set in sleep mode. The raw data transfer rate of the transceiver is 38.4 kbps; however, after incorporating a communication protocol, which includes a reliable retry-acknowledgement procedure, the effective data transfer rate is approximately 26 kbps. From the effective data transfer rate, it is estimated that if the sampling frequency of each sensor channel is 50 Hz, the central server is able to collect raw data from up to 24 sensing channels sampled continuously in real-time. The peer-to-peer communication capability of the wireless transceiver also makes it possible for the wireless sensing units to communicate with each other, thus supporting collaborative local data analysis.

2.4 *Power consumption*

Power consumption is another important issue to consider when selecting the hardware elements of a wireless sensing unit. While power consumption of each hardware component should be minimized, it must not be carried out at the expense of the functionalities needed by the wireless sensing unit. The power consumed by the wireless sensing unit is a function of the voltage and the amount of electrical current supplied to each component. All of the hardware components are internally referenced at 5 V. The active and standby electrical current for each component of the wireless sensing unit is listed in table 2. When the wireless sensing unit is active, it is collecting, interrogating or wirelessly transmitting sensor data. In contrast, the wireless sensing unit can be placed in a sleep state from which it can be easily awakened; when in sleep mode, the unit consumes minimal amount of electrical current (denoted as the standby current).

The wireless transceiver consumes the greatest amount of electrical power when active ($45\,\text{mA} \times 5\,\text{V} = 225\,\text{mW}$), which indicates the importance of minimizing the use of the wireless communication channel as a means of preserving battery energy (Lynch *et al.* 2004a). The total active current, I_{active}, of the wireless sensing unit prototype with the wireless transceiver in operation, as measured by a digital multimeter in the laboratory, is found to be 77 mA. The wireless sensing unit can operate on any power source providing at least 5.2 V of voltage potential. In the current prototype, five ordinary lithium AA batteries (Energizer L91), providing a total voltage of 7.5 V, are used. With the total energy capacity, E_{battery}, of a single L91 AA battery over 2900 mAh, the fully-active continuous life expectancy, T_{active}, of the wireless sensing unit is estimated to be:

$$T_{\text{active}} = \frac{E_{\text{battery}}}{I_{\text{active}}} = \frac{2900\,\text{mAh}}{77\,\text{mA}} = 37.7\,\text{hrs} = 1.57\ \text{days}.$$

This expected active life is conservative because the estimation assumes the unit is in continuous operation at all times. However, duty cycle usage of the battery allows for the internal cell chemistries to attain equilibrium and can thus extend batteries' life expectancies. The standby lifetime, T_{standby}, of the wireless sensing unit is:

$$T_{\text{standby}} = \frac{E_{\text{battery}}}{I_{\text{standby}}} = \frac{2900\,\text{mAh}}{100\,\mu\text{A}} = 29000\,\text{hrs} = 1208.3\ \text{days}.$$

In all likelihood, wireless sensing units serving as part of a comprehensive structural health monitoring system would be operated on a duty-cycle schedule. For example, units might be programmed to turn on every day for 10 minutes to measure the ambient response of the instrumented structure. If it is assumed that on each day, the system is fully active for 10 minutes for data collection and transmission, the total operation time of the wireless sensing unit unattended in the field is estimated to be:

$$\begin{aligned} T_{\text{10 min-active-per-day}} &= \frac{E_{\text{battery}}}{E_{\text{0.17 hr-active-per-day}} + E_{\text{23.83 hr-standby-per-day}}} \\ &= \frac{2900\,\text{mAh}}{77\,\text{mA} \times 0.17\,\text{hr/day} + 100\,\mu\text{A} \times 23.83\,\text{hr/day}} \\ &= 190\,\text{days}. \end{aligned}$$

If the unit is only used for 5 minutes every day, then the life expectancy of the unit is about one year.

Table 2. Approximate current consumption of the wireless sensing unit.

	Active current	Standby current
A/D converter ADS8341 (at 100 Hz)	1 mA	1 μA
Micro-controller ATmega128 (at 8 MHz)	15 mA	40 μA
SRAM CY62128B	15 mA	15 μA
Wireless transceiver 9XCite (TX/RX)	45 mA	20 μA
Support electronics	1 mA	24 μA
Total	77 mA	100 μA

2.5 *The assembled prototype wireless sensing unit*

For compact design of the wireless sensing unit, a simple two-layer printed circuit board (PCB) is designed and fabricated. A picture of the completed PCB, with integrated circuit chips attached, is shown in figure 2. The dimensions of the simple two-layer PCB are roughly 9.7×5.8 cm, which can further be reduced when using multi-layer PCB manufacturing. To protect the electronics from the harsh weather conditions common to outdoor structural applications, the PCB, wireless transceiver, and batteries are

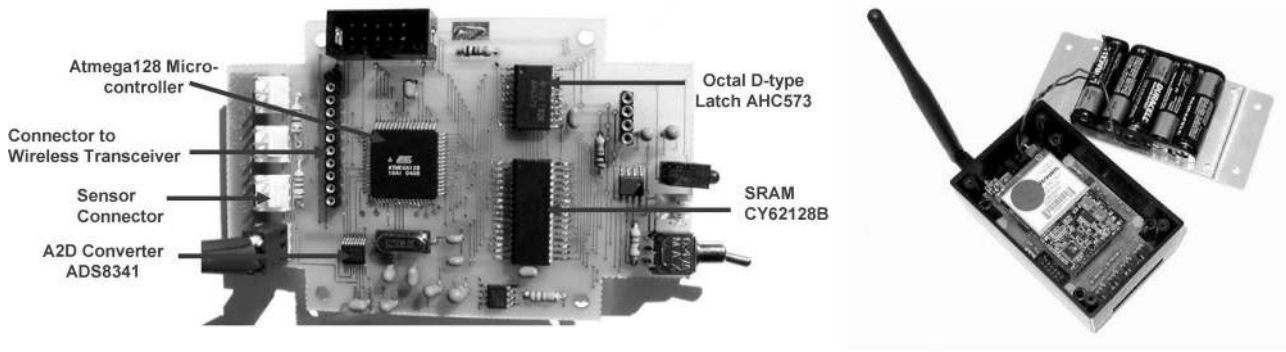

Figure 2. Printed circuit board and prototype packaging of the wireless sensing unit.

stored within a weatherproof plastic container. The figure also shows a picture of the prototype package that is opened to illustrate the internal components. The visible parts include the battery pack, the weatherproof container, the 9XCite wireless transceiver that is mounted on the PCB board, and the antenna of the wireless transceiver. The final dimensions of the wireless sensing unit (i.e. the plastic container) are $10.2 \times 6.5 \times 4.0$ cm.

3. Software design for the wireless SHM system

A simple star-topology wireless data acquisition system is designed and implemented in our current prototype SHM system. The system includes one central data server and multiple wireless sensing units. The central server is responsible for: (1) commanding all of the wireless sensing units to perform data collection tasks, (2) synchronizing the internal clocks of the wireless sensing units, (3) receiving data from the wireless network, and (4) storing the measurement data in a file server. Any desktop or laptop computer with a MaxStream 9XCite wireless transceiver connected can be used as the central server. Software written for the wireless structural monitoring system is divided into two parts: computer software for the central server, and embedded software for the wireless sensing units. Since the central server and the wireless sensing units must communicate frequently with one another, portions of their software are designed to allow seamless integration and coordination. A state diagram is constructed to describe in detail the program flow for both the central server and the wireless sensing unit. The intention of the state diagram is to encode a sequence of actions for both the central server and the wireless sensing units so that all potential problematic scenarios (or states) commonly encountered in an unreliable wireless channel can be efficiently handled.

In the prototype system, the central server is assigned the responsibility for ensuring reliable wireless communication. In other words, the central server plays an 'active' role in the communication channel while the wireless sensing unit plays more of a 'passive' role. For example, communication is always initiated by the central server. After the central server sends a command to the wireless sensing unit, if the server does not receive an expected response from the unit, the server will resend the last command again until the expected response is received. However, after a wireless sensing unit sends a message to the central server, the unit does not check if the message has arrived at the central server correctly or not, because the communication reliability is always guaranteed by the server. The wireless sensing unit only becomes aware of the lost data when the central server queries the unit for the same data again. This section describes the nature of the communication between the central server and the wireless sensing units, and the memory management mechanism implemented on the wireless sensing units that enables real-time continuous data collection by the central server from multiple wireless sensing units. The implementation of a local data processing algorithm in the current set of prototype wireless sensing units is also described in detail.

3.1 *Data synchronization*

For many damage and system identification procedures, measurement data individually collected by the different sensors must be time synchronized. For example, modal analysis and system identification algorithms usually require synchronized acceleration data from different locations of the structure (Ljung 1999, Ewins 2000). Figure 3 shows the design of the communication protocol between the central server and the wireless sensing units to accomplish clock synchronization.

The synchronization procedure utilizes the 9XCite wireless transceiver's point-to-multipoint communication capability. This feature permits the central data server's wireless transceiver to broadcast a beacon signal to which all wireless sensing units can synchronize. Once the wireless sensing units receive the beacon signal from the central server, each unit starts sampling the data at the requested

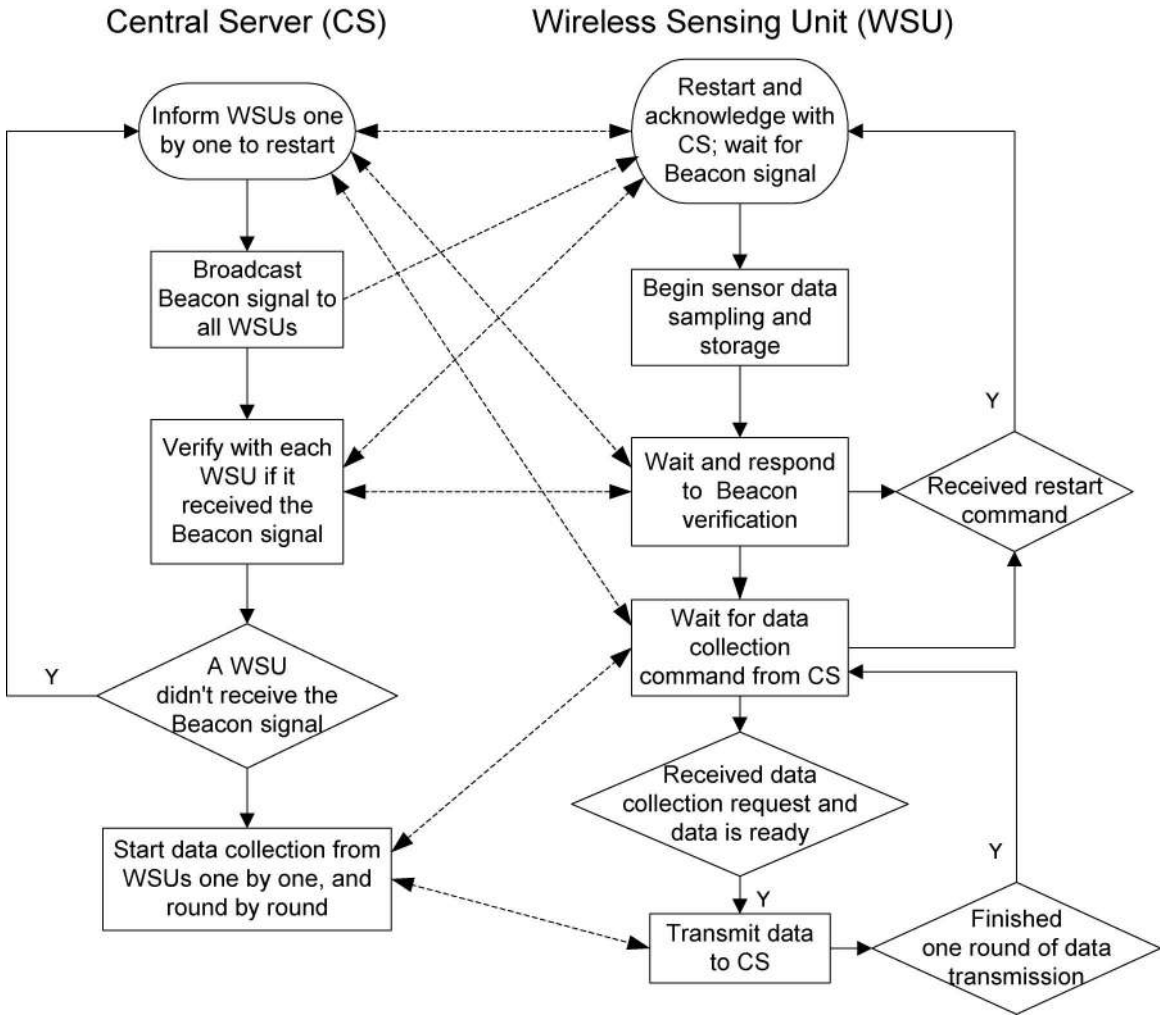

Figure 3. State diagram detailing the procedure for synchronizing the wireless sensing units.

rate. To account for the scenario where a wireless sensing unit might not receive the beacon signal, it is necessary for all wireless sensing units to confirm with the central server that they have received the beacon signal successfully. As shown in figure 3, when the central server inquires with a unit whether the unit has received the beacon signal, the server may be communicating with a unit that is still waiting for the beacon signal it has never received. If this happens, the central server restarts all of the wireless sensing units by asking them to wait for another beacon signal, and then re-broadcasts the beacon signal. The synchronization procedure is iterated until the central server has confirmed that the beacon signal has been received by all of the wireless sensing units in the network.

Although all the units can receive the same beacon signal from the central server, each wireless sensing unit may not receive the beacon at precisely the same time; therefore, some units may start collecting data slightly earlier while others may start slightly later. Because the propagation of the wireless radio-frequency (RF) signal takes only nanoseconds in this application, the synchronization error mainly originates from the difference in the time each wireless sensing unit takes to interpret the broadcasted beacon signal. Using precise timers in the laboratory, the synchronization error between two sensing units is measured to be within $20\,\mu$s of one another. This laboratory based timing of the synchronization error is intended to measure the expected error in a single-hop wireless sensor network installed in a civil structure within a short range to the central data repository (within 100 m). Because each wireless sensing unit is listening for the single central server beacon signal, time synchronization across the entire wireless sensor network is represented by uncoupled unit-server pairs. With one unit not dependent upon other units for time synchronization, the tests results encountered in the lab using two sensing units represents the synchronization error for an entire wireless SHM system, independent of the number of wireless sensing units installed.

However, it should be noted that although the system synchronization error is around 20 μs at the beginning of the data collection, the synchronization error might increase after long periods of time because of a natural time drift in the crystal clocks integrated with each wireless sensing unit. Current prototype unit employs a low-cost 8 MHz crystal to provide a system clock for the ATmega128 microcontroller. Laboratory tests show that the synchronization error between two units can accumulate up to 5 ms in a 6 minute period. Thus, synchronization error is considered minimal and reasonable within the realistic time period for data collection, and synchronization of the system should be carried out at certain time intervals.

3.2 *Communication protocol design and implementation using state machine concept*

A robust data acquisition software system should be sufficiently reliable and able to detect failures in the wireless communication channel and to recover from any communication failures encountered. Due to the system complexity needed to ensure the reliability of the wireless communication channel, the state machine concept (Tweed 1994) is employed for the software architecture for both the wireless sensing units and the central server. A state machine consists of a set of states and the definition of a set of transitions among these states. At any point in time, the state machine can only be in one of the possible states. In response to different events, the state machine transits between its discrete states. Figure 4 shows the abridged state diagram for the central server software, and figure 5 shows the abridged state diagram for the wireless sensing unit software. For simplicity, only the part of the communication state diagram for synchronizing wireless sensing units is presented, i.e. these two parts of the communication state diagrams describe the program flow in order to realize the synchronization procedure introduced in section 3.1. In the state diagrams shown in figures 4 and 5, each rectangle or circle with bold boundary lines stands for one possible state; lines with arrows represent state transitions. For each transition, the normal text above the horizontal line specifies the event/condition upon which the transition should happen, and the italic text below the horizontal line specifies the service/action to be completed during this transition.

When a wireless sensing unit is powered on, the unit starts from '***State0* Bootup**' in figure 5. Under 'no condition', the unit automatically initializes the memory space, and transits into '***State1* Wait for 00Start**', where the '00Start' is the beacon signal that is broadcasted from the central server to all of the wireless sensing units, requesting all units to start data collection simultaneously. Accordingly, when the data collection program at the central server starts running, as shown in figure 4, the server will automatically broadcast the '00Start' beacon signal which all of the wireless sensing units receive. As soon as the wireless sensing unit receives and recognizes the '00Start' beacon, the sensing unit starts collecting data from its associated sensors at a specified sampling rate, and saves the data temporarily into its external SRAM for later acquisition by the central server. If all the wireless sensing units are assumed to take the same amount of time to receive and recognize this '00Start' signal, then all the units start recording data at the same time, i.e. the data acquisition is synchronized.

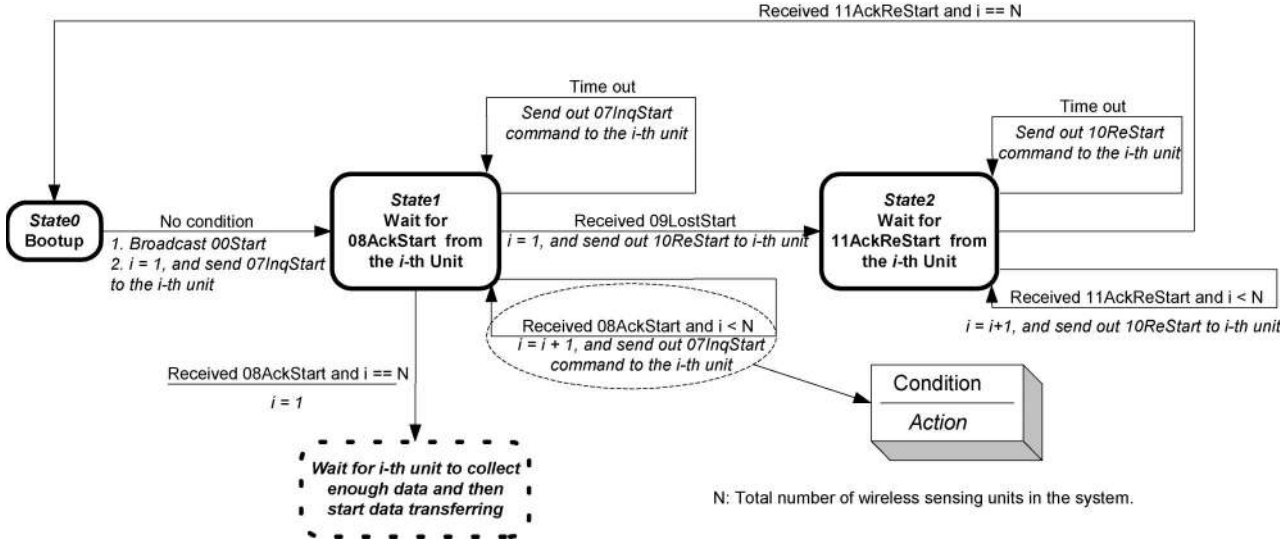

Figure 4. Abridged communication state diagram for the central server.

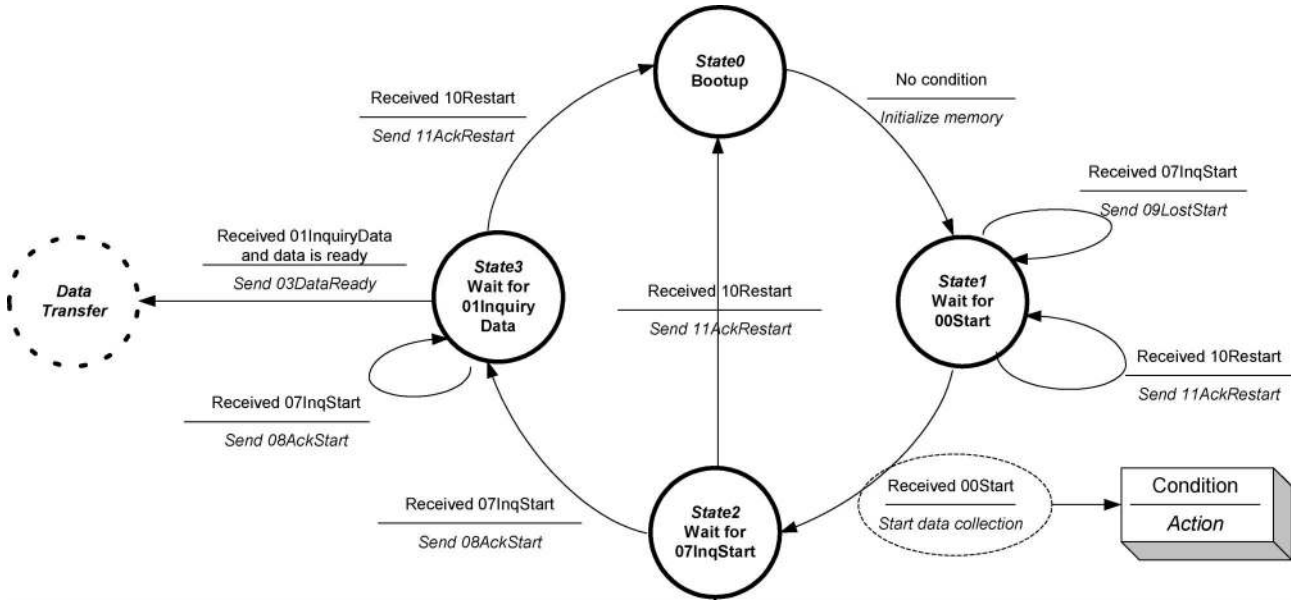

Figure 5. Abridged communication state diagram for the wireless sensing unit.

As shown in figure 5, after the wireless sensing unit receives the '00Start' command, it transits into '***State2* Wait for 07InqStart**'. Accordingly, after the central server broadcasts the '00Start' beacon signal, the server sends '07InqStart' to each unit, and waits until '08AckStart' message is returned from the sensing unit to confirm that this unit has received the '00Start' beacon. If any one of the wireless sensing units misses the '00Start' beacon, this unit will receive '07InqStart' command when itself is in '***State1***' (instead of in '***State2***'). In this case, the wireless sensing unit will send '09LostStart' in response to the central server's '07InqStart' inquiry. Knowing that the sensing unit has not properly received the '00Start' beacon, the central server will ask all of the units to restart and run the synchronization procedure again from the beginning, until the central server confirms that all the units have received the broadcasted '00Start' signal correctly.

As mentioned earlier, the central server is assigned the responsibility for ensuring the wireless communication channel is reliable (e.g. no data loss). To illustrate this, assume that in figure 5, when the wireless sensing unit transits from '***State2***' to '***State3***', the '08AckStart' message sent from the unit to the central server is lost. The central server is now at its '***State1***' waiting for the '08AckStart', but because the server cannot receive this '08AckStart' message within the certain expected time, the server will resend '07InqStart' to the unit. Therefore, in '***State3***' of the wireless sensing unit, although the unit should be waiting for the data acquisition request from the central server, the unit may still receive the '07InqStart' command because the last '08AckStart' was lost. In this case, the wireless sensing unit can handle this situation by simply resending '08AckStart' to the central server. This simple example illustrates the advantages inherent to the state machine concept when visualizing communication procedures. Although not presented here, the development of other facets of the communication protocol have demonstrated that the state machine concept provides the convenience for both designing and implementing program flow between the data server and the wireless sensing units.

3.3 *Real-time continuous data collection*

After the central server confirms that all of the wireless sensing units have received the latest beacon signal, the server starts inquiring the units one by one for the data they have thus far collected. Before the wireless sensing unit is queried for its data, the data is temporarily stored in the unit's onboard SRAM memory buffer. With over 128 kB of space available in memory, the wireless sensing unit can effectively store up to 64,000 data points (at 16 bit resolution). Once a unit is inquired by the server for measurement data, the wireless sensing unit transmits its most recently collected sensor data. A unique feature of the embedded wireless sensing unit software is that it can continue collecting data from interfaced sensors in real-time as the wireless sensing unit is transmitting data to the central server. The communication between the wireless sensing units and the central server during data transfer is highly reliable because of the network protocol in which the central server continues to request data from a unit until it receives the requested data.

At each instant in time, the central server can only communicate with one wireless sensing unit. In order to achieve real-time continuous data collection from multiple wireless sensing units with each unit having up to four analog sensors attached, a dual stack approach to managing the SRAM memory is taken in the current embedded software design. Essentially, the available memory bank of each unit is divided into four pairs of smaller memory stacks. When a wireless sensing unit starts collecting data, the embedded software establishes two memory stacks dedicated to each sensor channel for storing the sensor data. For each sensing channel, at any point of time, only one of the stacks is used to store the incoming data stream. During the procedure of storing new data into this memory stack, the system is responsible for sending the data in the other stack out to the central server. The role of each channel's two memory stacks alternates as soon as one stack is filled with newly collected data. Figure 6 illustrates the embedded system's management of the external SRAM memory. The two memory stacks, labeled 'Stacks "X"-1' and '"X"-2' for sensor channel "X" ("X" is 1 or 2 in this example), are shown in figure 6. In the diagram, incoming data from each sensor channel is stored in the second stack (denoted as 'Stacks 1-2' and '2-2') while the system is wirelessly transferring data from the first stack (denoted as 'Stacks 1-1' and '2-1'). Before 'Stacks "X"-2' are full, the wireless communication must be fast enough to transfer all the data from 'Stacks "X"-1'. After 'Stacks "X"-2' are filled with new data, the role of each pair of stacks alternates with the radio transmitting entries from 'Stacks "X"-2' and storing sensor data in 'Stacks "X"-1'.

The promptness of wireless communication is largely a function of the available wireless data transfer rate. In the current prototype system using the MaxStream 9XCite transceiver, the central server is able to collect raw data from up to 24 wireless sensors continuously in real-time with a sampling frequency of 50 Hz for each sensor, with the complete retry and acknowledgement communication protocol observed. As the sampling rate increases, the number of sensors that can be utilized decreases. For example, if a sampling rate of 100 Hz is desired, then only 12 sensors can be accommodated for real-time data communication with a single data server. If a high sampling rate and a large number of sensors are needed, then the system is not able to simultaneously collect data and wirelessly transmit at the same time. In such circumstances, the wireless sensing unit is first asked to collect a certain amount of data and to store the data temporarily in the

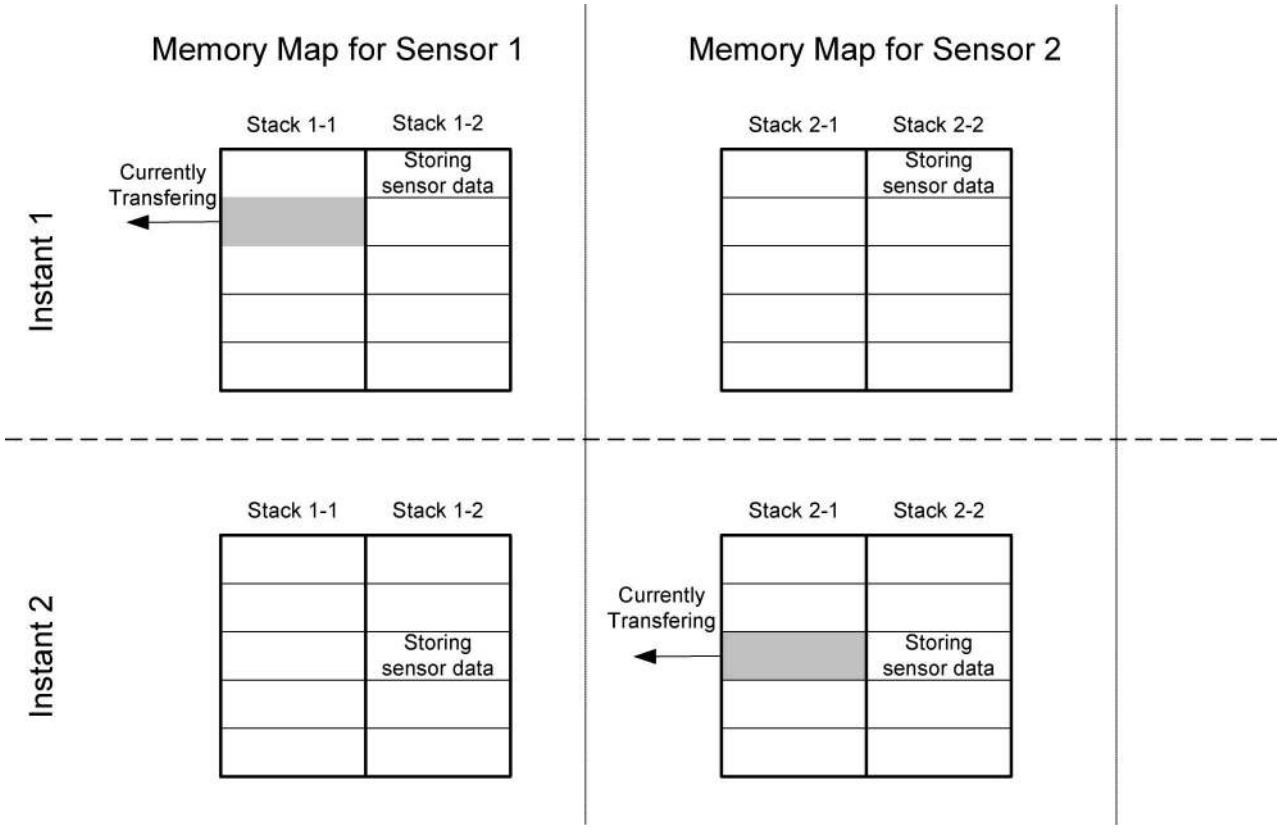

Figure 6. Dual-stack memory allocation for real-time continuous data collection.

local memory buffer. Upon completion, the wireless sensing unit can then send the data or the analysis results to the central server.

It should be noted that when the wireless sensing units are commanded to first store a certain period of data entirely before transmitting, the capacity of the wireless sensor network can be largely increased. Since in this configuration the demand for real-time delivery is not present, any sample rate can now be used. The only limitation encountered in this mode of operation is the available on-board memory which would control the duration of time the wireless sensor can collect data before exceeding its memory capacity.

3.4 *Fourier analysis using the wireless sensing unit*

To test the local data processing capability of the wireless sensing unit, a Fast Fourier Transform (FFT) algorithm using the Cooley-Turkey method (Press *et al*. 1992) is implemented and embedded in the core of the wireless sensing unit. Upon demand from the central server, the wireless sensing units can be commanded to collect sensor data and perform a floating-point FFT on the sampled data. After the FFT is calculated, the wireless sensing units would then wirelessly transfer either the complex valued FFT spectrum and/or the raw time-history data to the central server. Using the currently selected microcontroller and SRAM, a 4,096-point floating-point Cooley-Turkey FFT method takes about 18 seconds to complete. Within the wireless bandwidth limitation from the 9XCite wireless transceiver, if a 50 Hz sampling frequency is applied at each sensor, and only the FFT spectrum from 0 to 10 Hz is requested to be transferred back to the central server, the system can support real-time non-stop data collection and FFT results collection from up to 11 wireless sensing units simultaneously. Depending on the application, it may not be necessary to transfer the original time-history data. In that case, the number of units that are supported for simultaneous FFT analysis and results collection can be increased to approximately 25, if a 50 Hz sampling frequency is employed and a 0 to 10 Hz FFT spectrum is transferred from the wireless sensing units to the data server. In general, if the embedded local data processing algorithm is not computationally expensive and the size of the desired results to be transmitted is small, the number of wireless sensing units that can be supported for real-time data interrogation and simultaneous results transmission can be quite large.

4. Validation tests

To test the performance of the proposed wireless structural monitoring system, various validation tests are performed both in the laboratory and in the field. The results obtained from both sets of tests corroborate that the wireless sensing system is capable of accurately collecting data, performing data interrogation, and achieving reliable wireless communication. The field tests conducted at the Geumdang Bridge in Icheon, South Korea especially demonstrate the capability of the system to be applied to civil structures. This section presents in detail the results from the laboratory and field tests.

4.1 *Laboratory tests*

Laboratory tests of the wireless SHM system are devised using a three-story experimental structure. Figure 7 shows the aluminum structure employed in a shake-table test. Each floor of the structure weighs about 7.26 kg. The lateral stiffness of the structure is provided by four slender aluminum columns, each of which has a cross section of 0.64×1.27 cm. For theoretical computation, the three-story structure is simulated as a lumped-mass shear frame model. In another room about 15 meters away, a 9XCite wireless transceiver is connected with a computer so that it can serve as the central server for data acquisition. Two types of accelerometers are used for the validation test, showing the ability of the system to accommodate different analog sensors. A Crossbow CXL02LF1 accelerometer, which has an RMS (Root-Mean-Square) noise floor of 0.5 mg, is placed on the ground, the first, and the third floor, respectively. A Bosch SMB110 accelerometer, which has an RMS noise floor of 6.8 mg, is placed on the second floor.

In the first laboratory test, the structure is excited with a random initial velocity and displacement by the shake-table, then the shake-table stops moving and the structure vibrates freely. The wireless sensing unit associated with an accelerometer mounted on the third floor records the acceleration time history and transfers the data to the central server. Figure 8 shows the discrete Fourier transform (DFT) function corresponding to the measured acceleration time-history of the third-floor when the structure is under free vibration. The three natural frequencies extracted from the three peaks of the DFT plot are 2.07 Hz, 5.73 Hz, and 8.27 Hz, while the three theoretical natural frequencies computed from the simulation model are 2.08 Hz, 5.71 Hz, and 8.18 Hz respectively. The experimental and theoretical natural frequencies corroborate well, which underscores the accuracy of the acceleration time history collected by the wireless SHM system.

In the second laboratory test, the acceleration time history of each floor is measured when the structure is excited by a ground motion that is applied along the longitudinal direction of the structure. As shown in figure 7, accelerometers are placed on each floor including the ground level. An accelerometer is associated with each

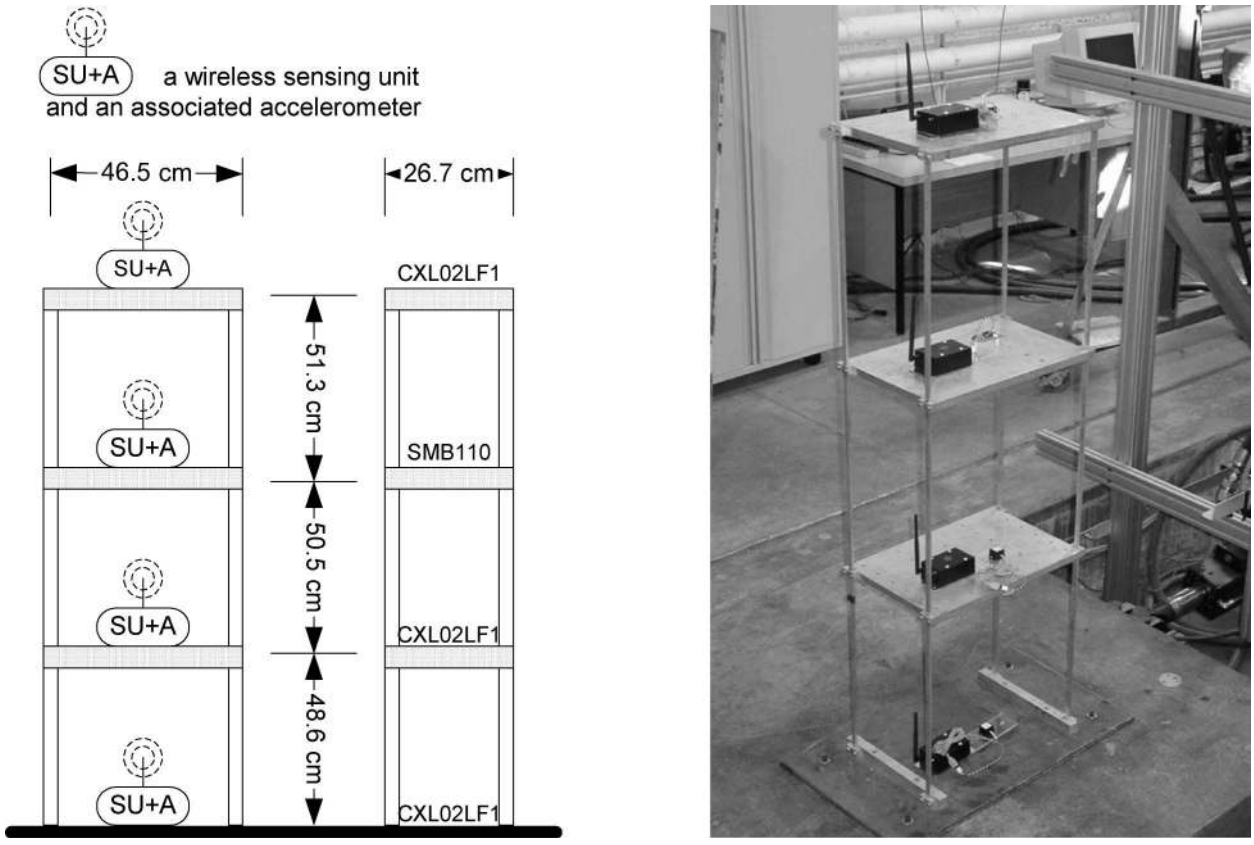

Figure 7. Test structure for laboratory validation of the wireless monitoring system.

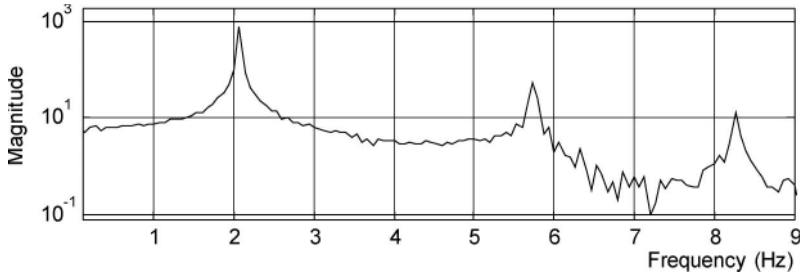

Figure 8. Discrete Fourier transform of the third-floor acceleration during free-vibration.

wireless sensing unit with each unit collecting data from the accelerometer at a sampling frequency of 200 Hz simultaneously to wirelessly transferring the data to the central server. Using the communication protocol designed earlier, the central server acquires near-synchronized dynamic data from all of the wireless sensing units in real-time.

The ground excitation for the second laboratory test is a chirping signal that has constant displacement amplitude with a linearly varying frequency. The actual ground acceleration time history is measured by the accelerometer and collected by the central server, as plotted in figure 9. The measurement shows that because the table excitation is not ideal, the actual ground acceleration measured at the ground level is noisy compared with an ideal chirping signal. Using the measured ground acceleration as input, the numerical simulation model is again executed to compute the theoretical response of the three floors by employing the average acceleration time integration method. A comparison between the measured and theoretical absolute acceleration time history at the third floor is shown in figure 10. The measured and the theoretical time history plots are similar in both shape and magnitude,

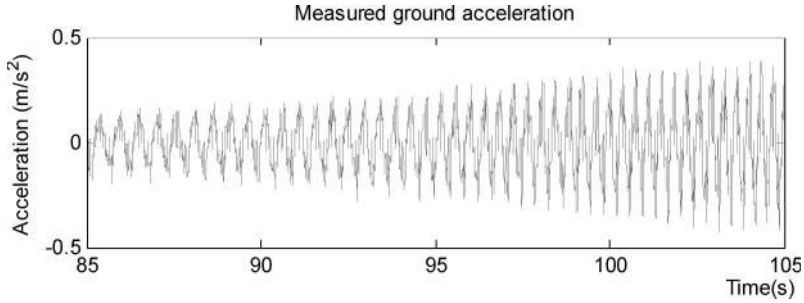

Figure 9. Ground acceleration time history for the laboratory test.

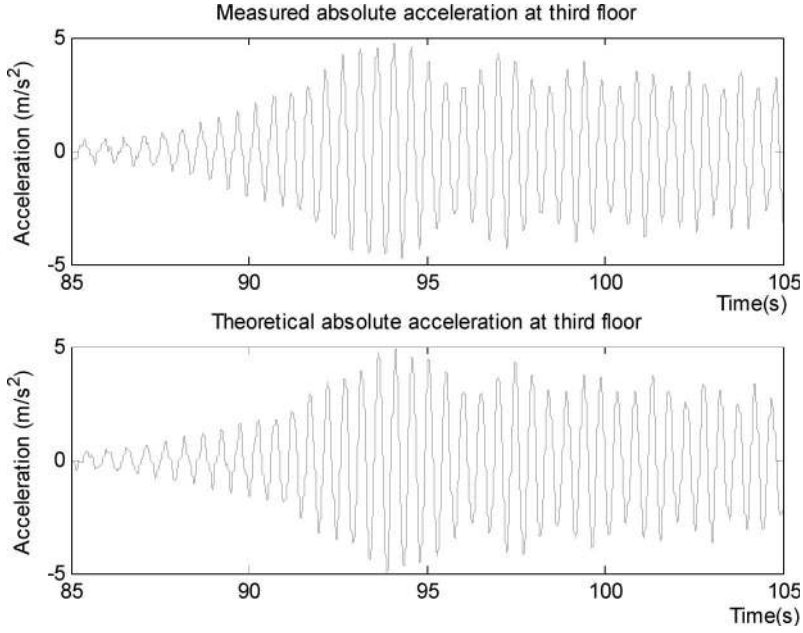

Figure 10. Comparison of measured and theoretical absolute acceleration at third floor.

which demonstrates the high quality of the data collected by the wireless monitoring system. Although the time history data at two other floors are not plotted, the measured and theoretical maximum absolute accelerations at each floor are presented in table 3. The difference between the maximum values at the second floor is slightly larger than the differences at the first and third floor. This is probably the result of differences in the performance of the two types of accelerometers.

Table 3. Comparison of measured and theoretical maximum absolute accelerations.

	1st floor	2nd floor	3rd floor
Measured (m/s^2)	2.14	3.35	4.74
Theoretical (m/s^2)	2.07	3.76	4.93
Relative Difference	3.32%	11.5%	3.93%

The third laboratory test is intended to measure the steady-state acceleration response of the structure under harmonic loading, and to use the wireless sensing unit to calculate the discrete Fourier transform of the acceleration response using the embedded FFT algorithm. Provided only the steady state behavior of the structure is recorded, the frequency response should contain energy mostly in the harmonic frequency of the shaking table. The shake-table is commanded to apply a harmonic base motion at a frequency of 5.7 Hz, which is close to the second natural frequency of the lumped-mass shear-frame structure. First, the three wireless sensing units installed in the structure at

each floor are employed to collect 4,096 data points at a sampling rate of 100 Hz after all dynamic response transients have died out. After collecting the acceleration response of the structure, the wireless sensing units then automatically calculate a 4096-point FFT using the acceleration response time-history of the structure. After the FFT computation, both the time history data and FFT results are transferred back to the central server for validation. Figure 11 illustrates the acceleration time history and FFT results computed by the wireless sensing units at the ground and at the third floor. Based on the FFT results calculated by the wireless sensing units, the frequency responses corresponding to the ground and third floor accelerations both have peak values at the frequency of 5.7 Hz, which matches well with the expectation for this experiment.

4.2 *Geumdang Bridge tests*

To test the performance of a large-scale wireless sensor network in a civil structure, field tests on the Geumdang Bridge in Icheon, South Korea are conducted. The Geumdang Bridge, a long-span concrete box girder bridge spanning 122 m, is instrumented with two sets of accelerometers attached to both a tethered and a wireless monitoring system. The depth of the box girder is 2.6 m while the top bridge deck has a total width of 12.6 m. The total span is supported along its length by three concrete piers and one concrete abutment. The locations of the piers along the span length are shown in figure 12.

Besides the wireless monitoring system, a wire-based structural monitoring system has also been installed. The wire-based system employs piezoelectric accelerometers to measure the vertical acceleration response of the bridge at the locations #1, 3, 4, 5, 6, 7, 8, 9, 10, 11, 13, 14, 15 and 16, as denoted in figure 12(a). The piezoelectric accelerometers used by the wire-based monitoring system are PCB393 accelerometers manufactured by PCB Piezotronics. For direct comparison, the wireless monitoring system also deploys accelerometers at these locations, with one accelerometer installed side-by-side to each PCB393 accelerometer. However, for the wireless monitoring system, lower-cost capacitive Piezotronics PCB3801 accelerometers are attached to the wireless sensing units at the 14 different sensor installation locations. Table 4 provides a performance comparison of the two accelerometers installed on the Geumdang Bridge. As illustrated in the table, PCB393 accelerometers used by the wire-based system have higher sensitivity and lower noise floors. Therefore, they are expected to have better performance than the PCB3801 accelerometers used by the wireless system. While the interior of the box girder protects the wireless sensing units from the natural elements, there are a number of vertical stiffener diaphragms within the box girder that attenuate the wireless signal between the wireless sensing units. The central server (laptop) is placed at the vicinity of sensor location #9, with a maximum distance between the central server and the furthest wireless sensing unit of about 60 m. As opposed to the wire-based system, installation of the wireless monitoring system takes

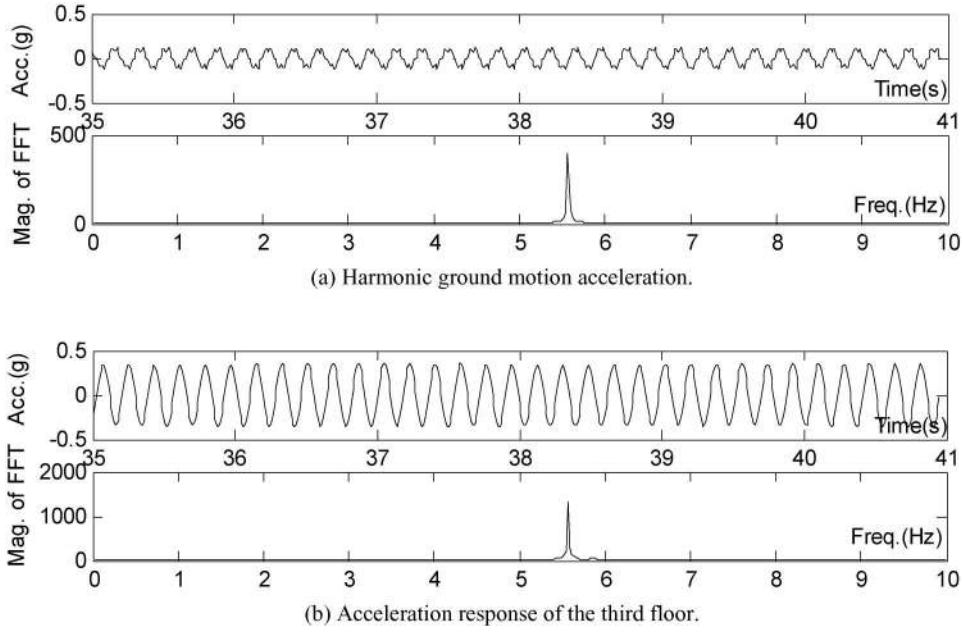

Figure 11. Acceleration time history measurements and the FFT results as computed by the wireless sensing units.

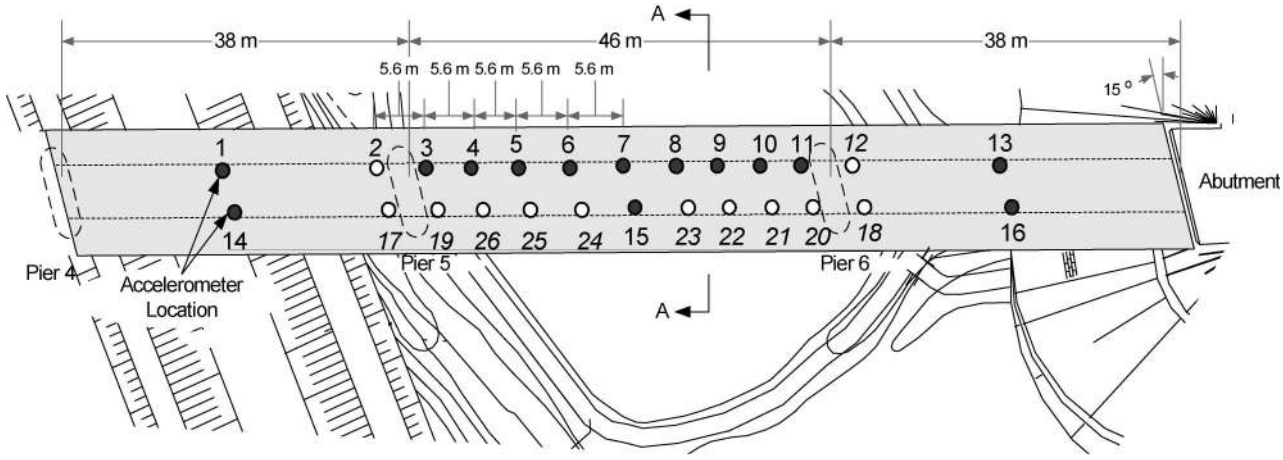

(a) Plan view showing tethered and wireless accelerometers placed side-by-side for 14 solid-dot locations.

(b) Outside perspective view of the bridge.

(c) Interior of the box girder.

Figure 12. Concrete box girder of the Geumdang Bridge in Icheon, South Korea.

Table 4. Performance comparison between accelerometers used by the wire-based and wireless systems.

	PCB393 (Wire-based system)	PCB3801 (Wireless system)
Sensor type	Piezoelectric	Capacitive
Maximum range	± 0.5 g	± 3 g
Sensitivity	10 V/g	0.7 V/g
Bandwidth	2000 Hz	80 Hz
RMS resolution (noise floor)	50 μg	500 μg
Minimal excitation voltage	18 VDC	5 VDC

only about one hour. For subsequent tests, the wireless sensing units are also moved around to different locations inside the box girder, a convenience made possible by using wireless communications.

For the wire-based monitoring system, the analog outputs of the PCB393 accelerometers are fed into a 16-channel PCB Piezotronics 481A03 signal conditioning unit. Before being sampled and digitized, the signals are amplified by a factor of 10 using an amplification circuit native to the signal conditioning unit. A National Instruments' 12 bit data acquisition card (model number 6062E) is used by a standard laptop computer to sample and digitize the amplified accelerometer signals. The wire-based monitoring system is configured to sample the 14 sensor channels at 200 Hz. For the wireless monitoring system, the PCB3801 accelerometers are connected directly to the sensing interface of each wireless sensing unit. Due to the limited wireless communication bandwidth and the large number of wireless sensing units that are streaming data simultaneously, the sampling rate of the wireless monitoring system is selected at 70 Hz. Over the course of two full

days of testing, the wireless monitoring system never experiences any communication problems including data losses. The designed communication protocol for near-synchronized and non-stop real-time data acquisition proves to be highly reliable for the wireless sensor deployment on the bridge structure.

The Geumdang Bridge is kept closed to regular highway traffic while the bridge is excited using trucks of known weight and speed crossing the bridge. Figure 13 illustrates the acceleration response of the bridge at sensor locations #8 and #13, when a 40-ton truck crosses the bridge at 60 km/h. Sensor #8 is near the central server, while sensor #13 is among the farthest units from the central server. The figure plots the acceleration time histories collected by the two different systems. A strong one-to-one correspondence exists in the acceleration response time history records collected by the two systems. As expected, the acceleration record measured by the wireless monitoring system appears noisier than that collected by the wire-based monitoring system, due to the difference in the accelerometers being used and the signal conditioning in the tethered system. The wireless sensing units are also commanded to perform a 4096 point FFT using the measured acceleration response. The frequency response as calculated by the wireless sensing unit is shown in figure 13. If the frequency response is compared to the frequency response calculated off-line using the response data collected by the wire-based monitoring system, again the FFT results from the two

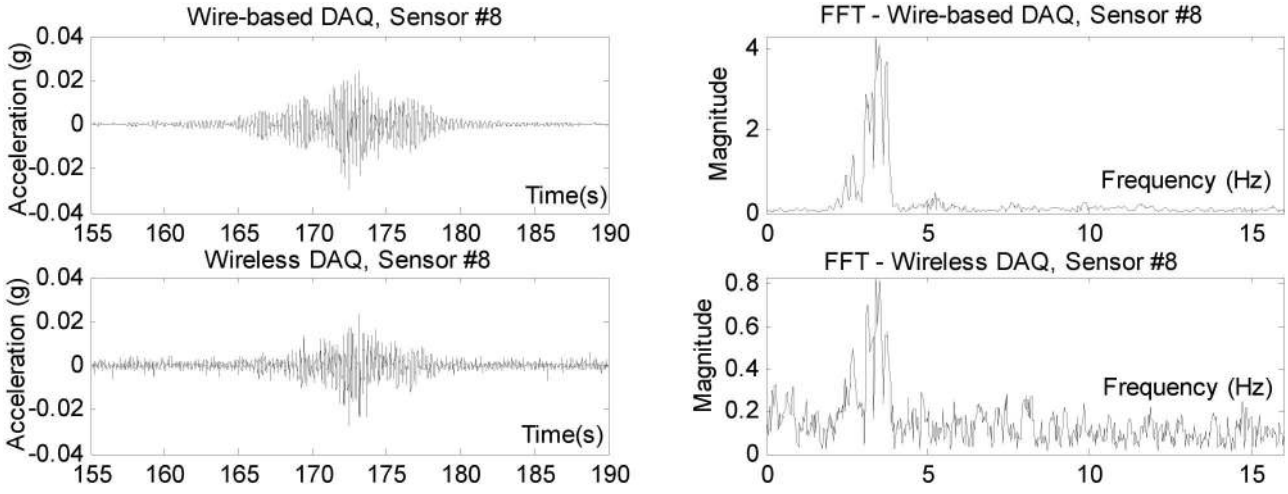

(a) Time-history responses and FFT results for sensor location #8.

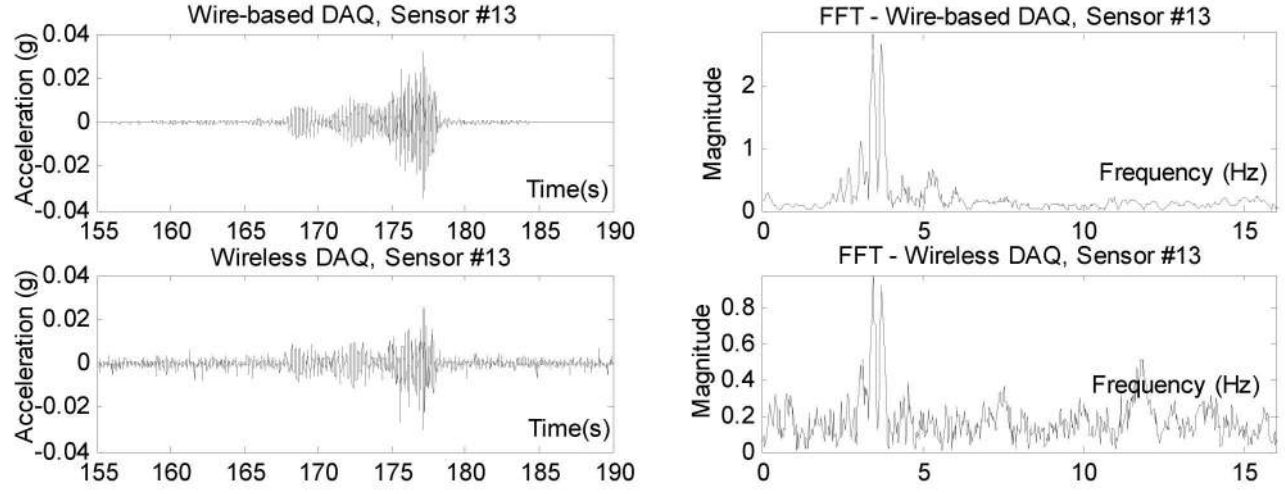

(b) Time-history responses and the FFT results for sensor location #13.

Figure 13. Measured acceleration time-history responses and the FFT results for Geumdang Bridge tests.

systems are very close to each other. The difference in the amplitude of FFT results is mainly caused by the different sampling frequencies used in the two systems.

5. Summary and discussion

This paper has presented in great detail, the design of an integrated software and hardware architecture for wireless structural health monitoring systems. Special features of the prototype wireless monitoring system include: (1) low power consumption without sacrificing long-range communication, (2) rapid system installation and low system costs, (3) reliable communication protocols ensuring lossless wireless communications, (4) multithreaded embedded software allowing for simultaneous data sampling and wireless communications, (5) high-precision time synchronization, and (6) local data processing capabilities integrated with the wireless sensing units. Both laboratory and field validation tests corroborate the capability and reliability of the prototype system for large-scale deployment in civil structures. It should be noted that the hardware components and the circuit design will likely be changed with new requirements and as microprocessor and wireless technologies advance. Nevertheless, the design and decision process as described in this paper will likely remain valid.

The prototype system can further be improved in a number of areas. With respect to the wireless sensing unit hardware design, sensor signal conditioning and anti-noise filters can be designed to improve the measurement fidelity of the wireless sensing units. With the rapid development in wireless communication technologies, wireless transceivers that support longer communication ranges and higher data rates while consuming less power should be pursued. Improvements can also be made with respect to the embedded software. For example, more advanced communication protocols are needed to organize very-large-scale wireless sensor networks with peer-to-peer connections. Local data compression algorithms can be incorporated to reduce wireless communication in the network, thereby improving the scalability of the system. Different decentralized damage detection and system identification algorithms that are suitable for embedment in the computational core of the wireless sensing units can be tested. In terms of application of the system to civil structures, while the Geumdang Bridge tests illustrate the potential and robustness of large-scale wireless structural monitoring systems to replace tethered monitoring systems, additional field studies are needed to further refine the design of the prototype system.

Acknowledgements

This research is partially funded by the National Science Foundation under grants CMS-9988909 (Stanford University) and CMS-0421180 (University of Michigan). The first author is supported by an Office of Technology Licensing Stanford Graduate Fellowship. Additional support was provided by the Rackham Grant and Fellowship Program at the University of Michigan. The authors would like to express their gratitude to Professors Chung Bang Yun and Jin Hak Yi, as well as Mr Chang Geun Lee, from the Korea Advanced Institute of Science and Technology (KAIST) for access to Geumdang Bridge. During this study, the authors have received valuable advice on the printed circuit board layout from Professor Ed Carryer of the Mechanical Engineering Department at Stanford University. The authors appreciate the generous assistance from the individuals acknowledged above.

References

Arms, S.W., Townsend, C.P., Galbreath, J.H. and Newhard, A.T., Wireless strain sensing networks, in *Proceedings of the 2nd European Workshop on Structural Health Monitoring*, Munich, Germany, July 7–9, 2004.

Callaway, E.H. Jr., *Wireless Sensor Networks: Architectures and Protocols*, 2004 (Auerbach: New York, USA).

Celebi, M., *Seismic Instrumentation of Buildings (with Emphasis on Federal Buildings)*, Report No. 0-7460-68170, US Geological Survey (USGS), Menlo Park, CA, USA, 2002.

Chang, P.C., Flatau, A. and Liu, S.C., Review paper: health monitoring of civil infrastructure. *Struct. Health Monit.*, 2003, **2**, 257–267.

Chase, S., The role of smart structures in managing an aging highway, Keynote Presentation in *SPIE 8th Annual International Symposium on Smart Structures and Materials*, Newport Beach, CA, USA, March 4–8, 2001.

Churchill, D.L., Hamel, M.J., Townsend, C.P. and Arms, S.W., Strain energy harvesting for wireless sensor networks, in *Proceedings of SPIE 10th Annual International Symposium on Smart Structures and Materials*, SPIE v. 5055, edited by V.K. Varadan and L.B. Kish, San Diego, CA, USA, pp. 319–327, March 2–6, 2003.

Culler, D.E. and Hong, W., Wireless sensor networks: introduction. *Commun. ACM*, 2004, **47**, 30–33.

Elgamal, A., Conte, J.P., Masri, S., Fraser, M., Fountain, T., Gupta, A., Trivedi, M. and El Zarki, M., Health monitoring framework for bridges and civil infrastructure, in *Proceedings of the 4th International Workshop on Structural Health Monitoring*, edited by F.-K. Chang, Stanford, CA, USA, pp. 123–130, September 15–17, 2003.

Ewins, D.J., *Modal Testing: Theory, Practice, and Application*, 2000 (Research Studies Press: Hertfordshire, England).

Farrar, C.R., Sohn, H., Hemez, F.M., Anderson, M.C., Bement, M.T., Cornwell, P.J., Doebling, S.W., Schultze, J.F., Lieven, N. and Robertson, A.N., *Damage Prognosis: Current Status and Future Needs*, Los Alamos National Laboratory Report LA-14051-MS, Los Alamos, NM, USA, July 2003.

Glaser, S.D., Some real-world applications of wireless sensor nodes, in *Proceedings of SPIE 11th Annual International Symposium on Smart Structures and Materials*, SPIE v. 5391, edited by S.C. Liu, San Diego, CA, USA, pp. 344–355, March 14–18, 2004.

Hill, J.L., System architecture for wireless sensor networks. Ph.D. Thesis, University of California, Berkeley, CA, 2003.

Kling, R.M., Intel mote: an enhanced sensor network node, in *Proceedings of International Workshop on Advanced Sensors, Structural Health Monitoring, and Smart Structures*, Keio University, Japan, November 10–11, 2003.

Kottapalli, V.A., Kiremidjian, A.S., Lynch, J.P., Carryer, E., Kenny, T.W., Law, K.H. and Lei, Y., Two-tiered wireless sensor network architecture for structural health monitoring, in *Proceedings of SPIE 10th Annual International Symposium on Smart Structures and Material*, SPIE v. 5057, edited by S.C. Liu, San Diego, CA, USA, pp. 8–19, March 2–6, 2003.

Lei, Y., Kiremidjian, A.S., Nair, K.K., Lynch, J.P. and Law, K.H., Time synchronization algorithms for wireless monitoring system, in *Proceedings of SPIE 10th Annual International Symposium on Smart Structures and Materials*, SPIE v. 5057, edited by S.C. Liu, San Diego, CA, USA, pp. 308–317, March 2–6, 2003.

Liu, S.C. and Tomizuka, M., Vision and strategy for sensors and smart structures technology research, in *Proceedings of the 4th International Workshop on Structural Health Monitoring*, edited by F.-K. Chang, Stanford, CA, USA, pp. 42–52, September 15–17, 2003.

Ljung, L., *System identification – Theory for the User*, 1999 (Prentice-Hall: New Jersey, USA).

Lynch, J.P., Overview of wireless sensors for real-time health monitoring of civil structures, in *the 4th International Workshop on Structural Control*, New York City, NY, USA, June 10–11, 2004.

Lynch, J.P., Sundararajan, A., Law, K.H., Kiremidjian, A.S., Kenny, T. and Carryer, E., Embedment of structural monitoring algorithms in a wireless sensing unit. *Struct. Eng. Mech.*, 2003, **15**, 285–297.

Lynch, J.P., Sundararajan, A., Law, K.H., Kiremidjian, A.S. and Carryer, E., Embedding damage detection algorithms in a wireless sensing unit for attainment of operational power efficiency. *Smart Mater. Struct.*, 2004, **13**, 800–810.

Lynch, J.P., Wang, Y., Law, K.H., Yi, J.H., Lee, C.G. and Yun, C.B., Validation of large-scale wireless structural monitoring system on the Geumdang Bridge, in *Proceedings of 9th International Conference on Structural Safety and Reliability*, Rome, Italy, June 19–23, 2005.

Mastroleon, L., Kiremidjian, A.S., Carryer, E. and Law, K.H., Design of a new power-efficient wireless sensor system for structural health monitoring, in *Proceedings of SPIE 9th Annual International Symposium on NDE for Health Monitoring and Diagnostics*, SPIE v. 5395, edited by S.R. Doctor, Y. Bar-Cohen, A.E. Aktan and H.F. Wu, San Diego, CA, USA, pp. 51–60, March 14–18, 2004.

Min, R., Bhardwaj, M., Cho, S.H., Shih, E., Sinha, A., Wang, A. and Chandrakasan, A., Low-power wireless sensor networks, in *Proceedings of 14th International Conference on VLSI Design*, Bangalore, India, January 3–7, 2001.

Moore, M., Phares, B., Graybeal, B., Rolander, D. and Washer, G., *Reliability of Visual Inspection for Highway Bridges*, Technical Report No. FHWA-RD-01-020, v. 1,US Department of Transportation - Federal Highway Administration, McLean, VA, USA, June 2001.

Ou, J.P., Li, H. and Yu, Y., Development and performance of wireless sensor network for structural health monitoring, in *Proceedings of SPIE 11th Annual International Symposium on Smart Structures and Materials*, SPIE v. 5391, edited by S.C. Liu, San Diego, CA, USA, pp. 765–773, March 14–18, 2004.

Press, W.H., Teukolsky, S.A., Vetterling, W.T. and Flannery, B.P., *Numerical Recipes in C: The Art of Scientific Computing*, 1992, (Cambridge University Press: Cambridge, UK).

Roundy, S.J., Energy Scavenging for Wireless Sensor Nodes with a Focus on Vibration to Electricity Conversion. PhD Thesis, University of California, Berkeley, CA, USA, 2003.

Shinozuka, M., Feng, M.Q., Chou, P., Chen, Y. and Park, C., MEMS-based wireless real-time health monitoring of bridges, in *the 3rd International Conference on Earthquake Engineering*, Nanjing, China, October 19–21, 2004.

Sodano, H.A., Inman, D.J. and Park, G., A review of power harvesting from vibration using piezoelectric materials. *Shock and Vibration Digest*, 2004, **36**, 197–205.

Sohn, H., Farrar, C.R., Hunter, N.F. and Worden, K., Structural health monitoring using statistical pattern recognition techniques. *J. Dyn. Syst.-T. ASME*, 2001, **123**, 706–711.

Spencer, B.F. Jr., Ruiz-Sandoval, M.E. and Kurata, N., Smart sensing technology: opportunities and challenges. *Struct. Control Health Monit.*, 2004, **11**, 349–368.

Stallings, J.M., Tedesco, J.W., El-Mihilmy, M. and McCauley, M., Field performance of FRP bridge repairs. *J. Bridge Engrg.*, 2000, **5**, 107–113.

Straser, E.G. and Kiremidjian, A.S., *A Modular, Wireless Damage Monitoring System for Structures*, Report No. 128, John A. Blume Earthquake Eng. Ctr., Dept. of Civil and Environmental Eng., Stanford Univ., Stanford, CA, USA, 1998.

Tweed, D., Designing real-time embedded software using state-machine concepts. *Circuit Cellar Ink*, 1994, **53**, 12–19.

Warneke, B. and Pister, K.S.J., MEMS for distributed wireless sensor networks, in *Proceedings of 9th International Conference on Electronics, Circuits and Systems*, Dubrovnik, Croatia, September 15–18, 2002.

Wang, Y., Lynch, J.P. and Law, K.H., Wireless structural sensors using reliable communication protocols for data acquisition and interrogation, in *Proceedings of the 23rd International Modal Analysis Conference (IMAC XXIII)*, Orlando, FL, January 31–February 3, 2005.

Wang, Y., Lynch, J.P. and Law, K.H., Design of a low-power wireless structural monitoring system for collaborative computational algorithms, in *Proceedings of SPIE 10th Annual International Symposium on Nondestructive Evaluation for Health Monitoring and Diagnostics*, San Diego, CA, March 6–10, 2005.